5. SOLUTION OF THE INCOMPRESSIBLE DRIVEN CAVITY PROBLEM BY THE ALTERNATING-DIRECTION IMPLICIT METHOD

Dana J. Morris
Langley Research Center

SUMMARY

A second-order accurate alternating-direction implicit (ADI) method has been used to solve the two-dimensional incompressible Navier-Stokes equations for flow in a square driven cavity. Calculations were made at a Reynolds number of 100 with equally spaced 15×15, 17×17, 33×33, and 57×57 grids and at a Reynolds number of 10 with a 15×15 grid. The ADI results agreed well with other solutions. Choosing a criterion for convergence which was too strict was found to result in no steady-state solution being reached. A study of the maximum allowable time step for a Reynolds number of 100 indicated that time steps many times larger than those used for most consistent explicit methods could be used for the ADI method.

INTRODUCTION

A second-order accurate efficient implicit method is used to solve the two-dimensional incompressible Navier-Stokes equations for flow in a square driven cavity. (See paper no. 1 by Rubin and Harris for details of the driven cavity problem.) This problem was previously solved by Mills (ref. 1) using an explicit method.

Alternating-direction implicit (ADI) methods were introduced by Peaceman and Rachford (ref. 2) and take advantage of a splitting of the time step for multidimensional problems to obtain an implicit method which requires only the inversion of a tridiagonal matrix. The expected unconditional stability of the method allowed larger time steps than explicit methods without the complexity of a full matrix reduction routine required by one-step implicit methods.

SYMBOLS

K	constant
Δl	$= \Delta x = \Delta y$
N	number of grid points in one direction

R	Reynolds number
Δt	time step
u	axial velocity component
v	normal velocity component
x,y	axial and normal coordinate, respectively
$\Delta x, \Delta y$	spatial increments in x- and y-directions
ζ	vorticity
ν	kinematic viscosity
ψ	stream function

Superscripts:

n	index of time step
*	intermediate time level

Subscripts:

i,j	index of grid point in x- and y-direction, respectively
t	differentiation with respect to time
w	value at wall
x,y	differentiation with respect to x or y

METHOD OF SOLUTION

The nondimensional equations for viscous incompressible two-dimensional flow in vorticity—stream-function form which describe the flow field under investigation are

$$\zeta_t = -u\zeta_x - v\zeta_y + \nu\zeta_{xx} + \nu\zeta_{yy} \tag{1}$$

$$\nabla^2\psi = \zeta \tag{2}$$

and $u = \psi_y$, $v = -\psi_x$, and $\nu = 1/R$.

Applied to the vorticity transport equation (eq. (1)), the Peaceman-Rachford (ref. 2) alternating-direction implicit (ADI) method advances one time level in the following two steps.

Step 1

$$\frac{\zeta^*_{i,j} - \zeta^n_{i,j}}{\Delta t/2} = -u\zeta^*_x - v\zeta_y{}^n + \nu\zeta^*_{xx} + \nu\zeta^n_{yy}$$

Step 2

$$\frac{\zeta^{n+1}_{i,j} - \zeta^*_{i,j}}{\Delta t/2} = -u\zeta^*_x - v\zeta^{n+1}_y + \nu\zeta^*_{xx} + \nu\zeta^{n+1}_{yy}$$

The value ζ^* has no physical meaning.

The method applied to the linear equation has a formal error of order $O\left[(\Delta t)^2,(\Delta x)^2,(\Delta y)^2\right]$. It is unconditionally stable and consistent. The full second-order accuracy of the method can be deteriorated by the nonlinear terms which should be evaluated as u^* and v^n for step 1 and as u^* and v^{n+1} for step 2. If the old values u^n and v^n are used, the formal error is $O\left[\Delta t,(\Delta x)^2,(\Delta y)^2\right]$. Briley (ref. 3) calculated u^n and v^n and, from the previous values u^{n-1} and v^{n-1}, linearly extrapolated forward to u^* and v^*. This procedure is stable and appeared second-order accurate; however, additional storage is required for ψ^{n-1}. Another procedure (refs. 4 and 5) is to iterate on the entire time step, either to convergence or for a predictor-corrector method. In either case the error is $O\left[(\Delta t)^2\right]$ and additional storage is required for ψ^{n+1}. It is also possible to calculate ψ^* after step 1 and to use u^* and v^* in step 2. Aziz and Hellums (ref. 5) examined these alternatives and found iteration on the full two steps to be the most accurate. The iteration required to obtain full second-order accuracy of the nonlinear terms may not be undesirable since some iteration is an advantage in achieving accurate boundary values for ζ.

Although a linear Von Neumann analysis shows the ADI procedure to be unconditionally stable, a survey of the literature indicates that the procedure may not be unconditionally stable for flows with high Reynolds numbers because of the Δt time lag of ζ_w. (See ref. 6.) The degree of convergence for ζ_w to obtain stability is problem dependent. For large Δt, convergence may be prohibited by nonlinear effects. Also, the program-

ing involved with complex boundaries effectively restricts the use of this method to rectangular regions.

The tridiagonal nature of the matrix to be solved, although much simpler than that in fully implicit one-step methods, requires diagonal dominance if error buildup is to be avoided in the matrix inversion. This is equivalent to imposing a restriction on cell Reynolds number.

In the present study, the ADI procedure was applied to the vorticity transport equation. Central differencing was used with equal mesh spacing and nonlinear terms were lagged a full time step. After completing a full time step calculation on vorticity, the stream-function equation was solved by a successive overrelaxation (SOR) routine and the boundary conditions were updated. (The SOR routine was identical with the one used in the previous paper by Hirsh (paper no. 4).) The vorticity was then calculated for a new time step, rather than being iterated at each time level to achieve a solution which was second-order accurate in time, since the interest in this study was in the steady-state solution.

BOUNDARY CONDITIONS

The no-slip condition requires that both u and v (the normal and tangential gradients of ψ) are zero at the stationary walls whereas at the moving wall u is unity. These conditions are treated by taking a row of image points at a distance $\Delta l = \Delta x = \Delta y$ outside the boundaries. These values can be related to the interior points by taking derivatives at the boundaries. Thus, the boundary conditions for ζ are:

on the stationary walls,

$$\zeta_w = \frac{2\psi_{\text{interior}}}{(\Delta l)^2}$$

at the moving wall,

$$\zeta_w = \frac{2(\Delta l + \psi_{\text{interior}})}{(\Delta l)^2}$$

The boundary value of ψ is zero on all boundaries. Initial conditions are zero everywhere except on the moving wall.

RESULTS

These calculations were made at a Reynolds number of 100 for a square $N \times N$ cavity for $N = 15$, 17, 33, and 57 and at a Reynolds number of 10 for $N = 15$. For $N = 17$, the problem was also computed with the conservation form of the equations and the values were found to be much more accurate, although the computer time to achieve a converged solution was approximately 2 times longer. As shown in table I, the maximum value of the stream function increases with the number of grid points toward the value 0.101 published by Burggraf (ref. 7). The vorticity ζ at the midpoint of the moving wall is also shown. For $N = 15$, the solution was identical with the one published by Mills (ref. 1) with a maximum stream function of 0.08742. Machine plots of the velocity vectors and the streamlines of this flow field are shown in figure 1. The calculated values of vorticity ζ and stream function ψ for $N = 57$ are presented in table II. In figure 2 the axial component of velocity u is depicted along a vertical line passing through the vortex center, and the calculated values are shown in table III for the three cases, $N = 15$ and 57 in nondivergence form and $N = 17$ in divergence form. Attempts to increase the accuracy of the nonconservation form by increasing the number of nodal points resulted in solutions which did not converge because of a convergence criterion which was too strict. The percentage difference between time levels $n + 1$ and n was used to check convergence. For $N = 15$ and 17, solutions were achieved with the convergence requirement set at 0.00005. For $N = 33$, this requirement was repeatedly made less stringent and was set at 0.001 before a converged solution was reached. Solutions for $N = 57$ did not require further weakening of this convergence criterion. This study was made for a time step $\Delta t = \Delta x$, the Courant-Friedrichs-Lewy condition for explicit methods. Decreasing the Reynolds number to 10 for $N = 15$ also forced the convergence requirement to be set at 0.001 and the time step to be decreased. No attempt was made to find the maximum allowable time step for this Reynolds number. For a Reynolds number of 100, however, such a study was made with the nonconservation form of the equations and the results are shown in figure 3. For $N = 15$, no solution would converge for Δt greater than $7\,\Delta x$. An N of 17 required that Δt be lowered to $5\,\Delta x$. Increasing N to 33 with $\Delta t = 5\,\Delta x$ resulted in the solution iterating in the SOR routine until the time limit on the computer was reached. Lowering the time step to $3\,\Delta x$ allowed the solution to converge. For $N = 57$, convergence in the SOR routine required that $\Delta t = \Delta x$. Thus the maximum allowable time step appears to vary not only as a function of Δx but also with the number of grid points used.

CONCLUSIONS

An alternating-direction implicit (ADI) method has been used to solve the two-dimensional incompressible Navier-Stokes equations for flow in a square driven cavity. The following conclusions may be drawn:

(1) The ADI technique, although not unconditionally stable as a linear Von Neumann analysis indicates, does allow time steps many times larger than most consistent explicit methods.

(2) Choosing a criterion for convergence which is too strict may result in no steady-state solution being reached.

REFERENCES

1. Mills, Ronald D.: Numerical Solutions of the Viscous Flow Equations for a Class of Closed Flows. J. Roy. Aeronaut. Soc., vol. 69, no. 658, Oct. 1965, pp. 714-718; Correction, vol. 69, no. 660, Dec. 1965, p. 880.

2. Peaceman, D. W.; and Rachford, H. H., Jr.: The Numerical Solution of Parabolic and Elliptic Differential Equations. J. Soc. Ind. & Appl. Math., vol. 3, no. 1, Mar. 1955, pp. 28-41.

3. Briley, W. Roger: A Numerical Study of Laminar Separation Bubbles Using the Navier-Stokes Equations. J. Fluid Mech., vol. 47, pt. 4, June 1971, pp. 713-736.

4. Pearson, Carl E.: A Computational Method for Viscous Flow Problems. J. Fluid Mech. vol. 21, pt. 4, Apr. 1965, pp. 611-622.

5. Aziz, K.; and Hellums, J. D.: Numerical Solution of the Three-Dimensional Equations of Motion for Laminar Natural Convection. Phys. Fluids, vol. 10, no. 2, Feb. 1967, pp. 314-324.

6. Roache, Patrick J.: Computational Fluid Dynamics. Hermosa Publ., c.1972.

7. Burggraf, Odus R.: Analytical and Numerical Studies of the Structure of Steady Separated Flows. J. Fluid Mech., vol. 24, pt. 1, Jan. 1966, pp. 113-151.

TABLE I.- RESULTS FOR R = 100

N	Vorticity at midpoint of moving wall	Maximum stream function
15	8.9160	-0.08742
17	8.4646	-.09098
[a]17	7.3756	-.09867
33	6.9919	-.10038
57	6.6960	-.10128

[a]Divergence form.

TABLE II.- CALCULATED VORTICITY AND STREAM FUNCTION FOR SQUARE CAVITY WITH $R = 100$ AND EQUALLY SPACED 57×57 GRID

(a) Stream function

y	Stream function at x of –													
	0	0.0714	0.1428	0.2143	0.2857	0.3571	0.4286	0.5000	0.5714	0.6428	0.7143	0.7857	0.8571	0.9286	1.0
1.0000	0	0	0	0	0	0	0	0	0	0	0	0	0	0	0
.9286	0	-1.555×10^{-2}	-2.985×10^{-2}	-3.863×10^{-2}	-4.455×10^{-2}	-4.888×10^{-2}	-5.213×10^{-2}	-5.448×10^{-2}	-5.589×10^{-2}	-5.619×10^{-2}	-5.506×10^{-2}	-5.189×10^{-2}	-4.512×10^{-2}	-2.856×10^{-2}	0
.8571	0	-1.037×10^{-2}	-2.759×10^{-2}	-4.316×10^{-2}	-5.604×10^{-2}	-6.659×10^{-2}	-7.509×10^{-2}	-8.156×10^{-2}	-8.571×10^{-2}	-8.695×10^{-2}	-8.429×10^{-2}	-7.604×10^{-2}	-5.876×10^{-2}	-3.713×10^{-2}	0
.7857	0	-7.670×10^{-3}	-2.361×10^{-2}	-4.101×10^{-2}	-5.726×10^{-2}	-7.156×10^{-2}	-8.358×10^{-2}	-9.290×10^{-2}	-9.880×10^{-2}	-1.002×10^{-1}	-9.549×10^{-2}	-8.223×10^{-2}	-5.724×10^{-2}	-2.180×10^{-2}	0
.7143	0	-6.410×10^{-3}	-2.088×10^{-2}	-3.810×10^{-2}	-5.553×10^{-2}	-7.097×10^{-2}	-8.442×10^{-2}	-9.476×10^{-2}	-1.009×10^{-1}	-1.013×10^{-1}	-9.402×10^{-2}	-7.683×10^{-2}	-4.876×10^{-2}	-1.634×10^{-2}	0
.6428	0	-5.600×10^{-3}	-1.860×10^{-2}	-3.465×10^{-2}	-5.115×10^{-2}	-6.656×10^{-2}	-7.976×10^{-2}	-8.959×10^{-2}	-9.467×10^{-2}	-9.334×10^{-2}	-8.378×10^{-2}	-6.476×10^{-2}	-3.789×10^{-2}	-1.156×10^{-2}	0
.5714	0	-4.850×10^{-3}	-1.618×10^{-2}	-3.041×10^{-2}	-4.522×10^{-2}	-5.911×10^{-2}	-7.083×10^{-2}	-7.908×10^{-2}	-8.243×10^{-2}	-7.932×10^{-2}	-6.853×10^{-2}	-5.014×10^{-2}	-2.737×10^{-2}	-7.770×10^{-3}	0
.5000	0	-4.020×10^{-3}	-1.348×10^{-2}	-2.542×10^{-2}	-3.790×10^{-2}	-4.952×10^{-2}	-5.905×10^{-2}	-6.524×10^{-2}	-6.676×10^{-2}	-6.247×10^{-2}	-5.189×10^{-2}	-3.608×10^{-2}	-1.859×10^{-2}	-4.970×10^{-3}	0
.4286	0	-3.130×10^{-3}	-1.057×10^{-2}	-2.002×10^{-2}	-2.988×10^{-2}	-3.894×10^{-2}	-4.610×10^{-2}	-5.025×10^{-2}	-5.037×10^{-2}	-4.579×10^{-2}	-3.662×10^{-2}	-2.434×10^{-2}	-1.194×10^{-2}	-3.030×10^{-3}	0
.3571	0	-2.250×10^{-3}	-7.680×10^{-3}	-1.464×10^{-2}	-2.191×10^{-2}	-2.849×10^{-2}	-3.347×10^{-2}	-3.599×10^{-2}	-3.535×10^{-2}	-3.126×10^{-2}	-2.415×10^{-2}	-1.542×10^{-2}	-7.230×10^{-3}	-1.740×10^{-3}	0
.2857	0	-1.440×10^{-3}	-5.030×10^{-3}	-9.720×10^{-3}	-1.464×10^{-2}	-1.905×10^{-2}	-2.225×10^{-2}	-2.365×10^{-2}	-2.281×10^{-2}	-1.968×10^{-2}	-1.473×10^{-2}	-9.050×10^{-3}	-4.050×10^{-3}	-9.100×10^{-4}	0
.2143	0	-7.700×10^{-4}	-2.820×10^{-3}	-5.600×10^{-3}	-8.550×10^{-3}	-1.117×10^{-2}	-1.304×10^{-2}	-1.375×10^{-2}	-1.308×10^{-2}	-1.104×10^{-2}	-8.020×10^{-3}	-4.720×10^{-3}	-1.980×10^{-3}	-3.900×10^{-4}	0
.1428	0	-3.000×10^{-4}	-1.210×10^{-3}	-2.510×10^{-3}	-3.930×10^{-3}	-5.200×10^{-3}	-6.100×10^{-3}	-6.420×10^{-3}	-6.040×10^{-3}	-5.010×10^{-3}	-3.520×10^{-3}	-1.950×10^{-3}	-7.200×10^{-4}	-1.000×10^{-4}	0
.0714	0	-4.000×10^{-5}	-2.700×10^{-4}	-6.200×10^{-4}	-1.020×10^{-3}	-1.380×10^{-3}	-1.630×10^{-3}	-1.730×10^{-3}	-1.620×10^{-3}	-1.310×10^{-3}	-8.900×10^{-4}	-4.400×10^{-4}	-1.200×10^{-4}	-1.000×10^{-5}	0
0	0	0	0	0	0	0	0	0	0	0	0	0	0	0	0

TABLE II.- CALCULATED VORTICITY AND STREAM FUNCTION FOR SQUARE CAVITY WITH R = 100 AND EQUALLY SPACED 57 × 57 GRID – Concluded

(b) Vorticity

y	Vorticity at x of –														
	0	0.0714	0.1428	0.2143	0.2857	0.3571	0.4286	0.5000	0.5714	0.6428	0.7143	0.7857	0.8571	0.9286	1.0
1.0000			$2.099 \times 10^{+1}$	$1.495 \times 10^{+1}$	$1.159 \times 10^{+1}$	$9.338 \times 10^{+0}$	$7.749 \times 10^{+0}$	$6.696 \times 10^{+0}$	$6.187 \times 10^{+0}$	$6.317 \times 10^{+0}$	$7.254 \times 10^{+0}$	$9.314 \times 10^{+0}$	$1.345 \times 10^{+1}$	$2.537 \times 10^{+1}$	
.9286	$-1.291 \times 10^{+1}$	$2.644 \times 10^{+0}$	$6.096 \times 10^{+0}$	$6.718 \times 10^{+0}$	$6.603 \times 10^{+0}$	$6.287 \times 10^{+0}$	$5.937 \times 10^{+0}$	$5.624 \times 10^{+0}$	$5.393 \times 10^{+0}$	$5.296 \times 10^{+0}$	$5.418 \times 10^{+0}$	$5.969 \times 10^{+0}$	$7.587 \times 10^{+0}$	$9.314 \times 10^{+0}$	$-1.784 \times 10^{+1}$
.8571	$-5.622 \times 10^{+0}$	$-1.630 \times 10^{+0}$	4.408×10^{-1}	$1.520 \times 10^{+0}$	$2.198 \times 10^{+0}$	$2.683 \times 10^{+0}$	$3.072 \times 10^{+0}$	$3.421 \times 10^{+0}$	$3.764 \times 10^{+0}$	$4.128 \times 10^{+0}$	$4.561 \times 10^{+0}$	$5.184 \times 10^{+0}$	$5.861 \times 10^{+0}$	$1.160 \times 10^{+0}$	$-1.650 \times 10^{+1}$
.7857	$-3.662 \times 10^{+0}$	$-1.808 \times 10^{+0}$	-4.909×10^{-1}	3.429×10^{-1}	9.494×10^{-1}	$1.466 \times 10^{+0}$	$1.960 \times 10^{+0}$	$2.463 \times 10^{+0}$	$2.989 \times 10^{+0}$	$3.544 \times 10^{+0}$	$4.118 \times 10^{+0}$	$4.574 \times 10^{+0}$	$3.743 \times 10^{+0}$	$-2.257 \times 10^{+0}$	$-1.176 \times 10^{+1}$
.7143	$-2.955 \times 10^{+0}$	$-1.625 \times 10^{+0}$	-5.830×10^{-1}	1.401×10^{-1}	6.891×10^{-1}	$1.180 \times 10^{+0}$	$1.673 \times 10^{+0}$	$2.191 \times 10^{+0}$	$2.729 \times 10^{+0}$	$3.262 \times 10^{+0}$	$3.674 \times 10^{+0}$	$3.538 \times 10^{+0}$	$1.563 \times 10^{+0}$	$-3.278 \times 10^{+0}$	$-7.588 \times 10^{+0}$
.6428	$-2.565 \times 10^{+0}$	$-1.429 \times 10^{+0}$	-5.405×10^{-1}	9.230×10^{-2}	5.837×10^{-1}	$1.036 \times 10^{+0}$	$1.499 \times 10^{+0}$	$1.981 \times 10^{+0}$	$2.448 \times 10^{+0}$	$2.817 \times 10^{+0}$	$2.876 \times 10^{+0}$	$2.133 \times 10^{+0}$	-7.014×10^{-2}	$-3.180 \times 10^{+0}$	$-4.996 \times 10^{+0}$
.5714	$-2.218 \times 10^{+0}$	$-1.235 \times 10^{+0}$	-4.834×10^{-1}	4.798×10^{-2}	4.615×10^{-1}	8.450×10^{-1}	$1.235 \times 10^{+0}$	$1.620 \times 10^{+0}$	$1.941 \times 10^{+0}$	$2.074 \times 10^{+0}$	$1.795 \times 10^{+0}$	7.996×10^{-1}	-9.464×10^{-1}	$-2.610 \times 10^{+0}$	$-3.164 \times 10^{+0}$
.5000	$-1.836 \times 10^{+0}$	$-1.035 \times 10^{+0}$	-4.318×10^{-1}	-1.229×10^{-2}	3.092×10^{-1}	6.012×10^{-1}	8.847×10^{-1}	$1.134 \times 10^{+0}$	$1.281 \times 10^{+0}$	$1.209 \times 10^{+0}$	7.721×10^{-1}	-1.050×10^{-1}	$-1.199 \times 10^{+0}$	$-1.931 \times 10^{+0}$	$-1.921 \times 10^{+0}$
.4286	$-1.421 \times 10^{+0}$	-8.311×10^{-1}	-3.863×10^{-1}	-8.093×10^{-2}	1.470×10^{-1}	3.443×10^{-1}	5.181×10^{-1}	6.401×10^{-1}	6.516×10^{-1}	4.793×10^{-1}	7.067×10^{-2}	-5.260×10^{-1}	$-1.091 \times 10^{+0}$	$-1.325 \times 10^{+0}$	$-1.112 \times 10^{+0}$
.3571	$-1.004 \times 10^{+0}$	-6.322×10^{-1}	-3.435×10^{-1}	-1.462×10^{-1}	-3.450×10^{-3}	1.126×10^{-1}	2.018×10^{-1}	2.388×10^{-1}	1.865×10^{-1}	1.356×10^{-2}	-2.761×10^{-1}	-6.029×10^{-1}	-8.463×10^{-1}	-8.533×10^{-1}	-6.003×10^{-1}
.2857	-6.233×10^{-1}	-4.492×10^{-1}	-3.008×10^{-1}	-1.995×10^{-1}	-1.298×10^{-1}	-7.603×10^{-1}	-4.025×10^{-2}	-4.022×10^{-2}	-9.653×10^{-2}	-2.169×10^{-1}	-3.807×10^{-1}	-5.323×10^{-1}	-5.961×10^{-1}	-5.159×10^{-1}	-2.831×10^{-1}
.2143	-3.115×10^{-1}	-2.927×10^{-1}	-2.572×10^{-1}	-2.367×10^{-1}	-2.292×10^{-1}	-2.241×10^{-1}	-2.203×10^{-1}	-2.275×10^{-1}	-2.572×10^{-1}	-3.114×10^{-1}	-3.745×10^{-1}	-4.146×10^{-1}	-3.950×10^{-1}	-2.900×10^{-1}	-9.135×10^{-2}
.1428	-9.455×10^{-2}	-1.711×10^{-1}	-2.124×10^{-1}	-2.567×10^{-1}	-3.051×10^{-1}	-3.453×10^{-1}	-3.685×10^{-1}	-3.755×10^{-1}	-3.722×10^{-1}	-3.632×10^{-1}	-3.464×10^{-1}	-3.127×10^{-1}	-2.504×10^{-1}	-1.481×10^{-1}	1.013×10^{-2}
.0714	-6.710×10^{-3}	-8.313×10^{-2}	-1.608×10^{-1}	-2.579×10^{-1}	-3.635×10^{-1}	-4.559×10^{-1}	-5.163×10^{-1}	-5.328×10^{-1}	-5.029×10^{-1}	-4.331×10^{-1}	-3.375×10^{-1}	-2.339×10^{-1}	-1.339×10^{-1}	-5.867×10^{-2}	2.978×10^{-2}
0	0	6.610×10^{-3}	-8.180×10^{-2}	-2.378×10^{-1}	-4.141×10^{-1}	-5.763×10^{-1}	-6.946×10^{-1}	-7.403×10^{-1}	-6.929×10^{-1}	-5.532×10^{-1}	-3.528×10^{-1}	-1.498×10^{-1}	-8.960×10^{-3}	2.866×10^{-2}	0

TABLE III. - RESULTS FOR VELOCITY COMPONENT u THROUGH POINT OF MAXIMUM STREAM FUNCTION FOR R = 100

y	u through point of maximum ψ with –		
	15 × 15 grid, nondivergence form	57 × 57 grid, nondivergence form	17 × 17 grid, divergence form
0	0	0	0
.0625	----------	----------	-3.509×10^{-2}
.0714	-2.612×10^{-2}	-3.556×10^{-2}	----------
.1250	----------	----------	-6.513×10^{-2}
.1428	-5.018×10^{-2}	-6.774×10^{-2}	----------
.1875	----------	----------	-9.419×10^{-2}
.2143	-7.583×10^{-2}	-1.019×10^{-1}	----------
.2500	----------	----------	-1.245×10^{-1}
.2857	-1.054×10^{-1}	-1.409×10^{-1}	----------
.3125	----------	----------	-1.563×10^{-1}
.3571	-1.388×10^{-1}	-1.834×10^{-1}	----------
.3750	----------	----------	-1.868×10^{-1}
.4286	-1.724×10^{-1}	-2.215×10^{-1}	----------
.4375	----------	----------	-2.107×10^{-1}
.5000	-1.968×10^{-1}	-2.404×10^{-1}	-2.198×10^{-1}
.5625	----------	----------	-2.057×10^{-1}
.5714	-1.980×10^{-1}	-2.233×10^{-1}	----------
.6250	----------	----------	-1.622×10^{-1}
.6429	-1.616×10^{-1}	-1.606×10^{-1}	----------
.6875	----------	----------	-8.745×10^{-2}
.7143	-7.891×10^{-2}	-5.416×10^{-2}	----------
.7500	----------	----------	1.782×10^{-2}
.7857	5.022×10^{-2}	9.200×10^{-2}	----------
.8125	----------	----------	1.578×10^{-1}
.8571	2.445×10^{-1}	2.929×10^{-1}	----------
.8750	----------	----------	3.519×10^{-1}
.9286	5.470×10^{-1}	5.905×10^{-1}	----------
.9375	----------	----------	6.315×10^{-1}
1.0000	1.0	1.0	1.0

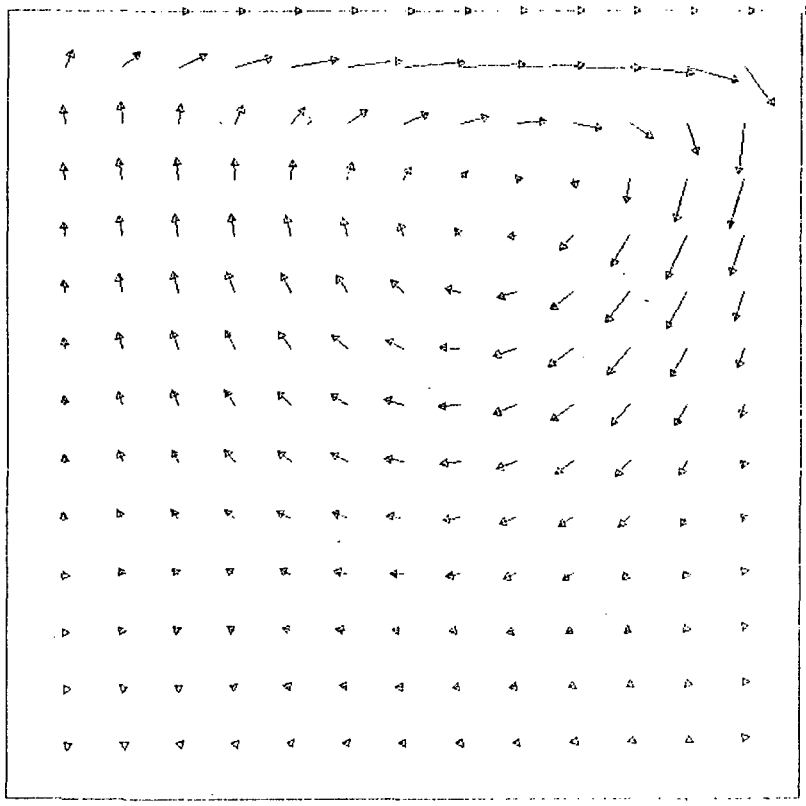

(a) Velocity vectors.

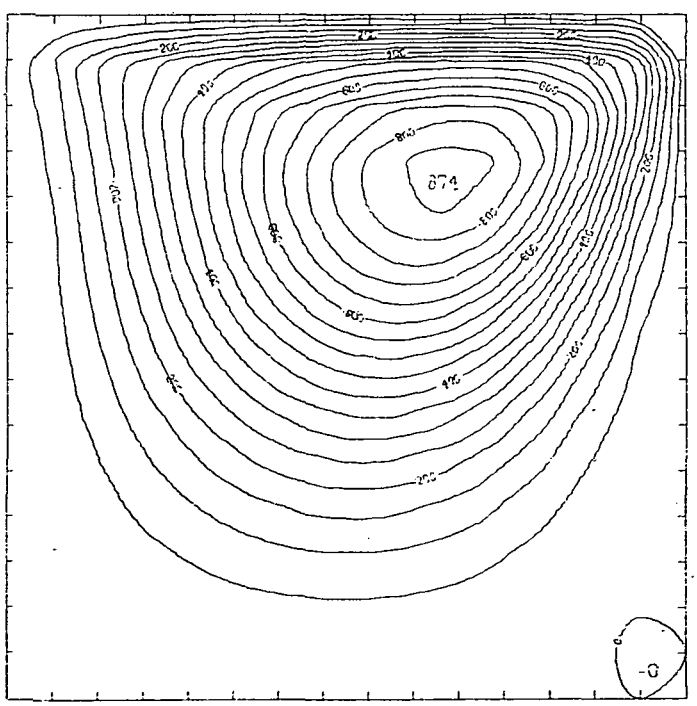

(b) Streamlines.

Figure 1.- Machine plots of flow field. N = 15; R = 100.

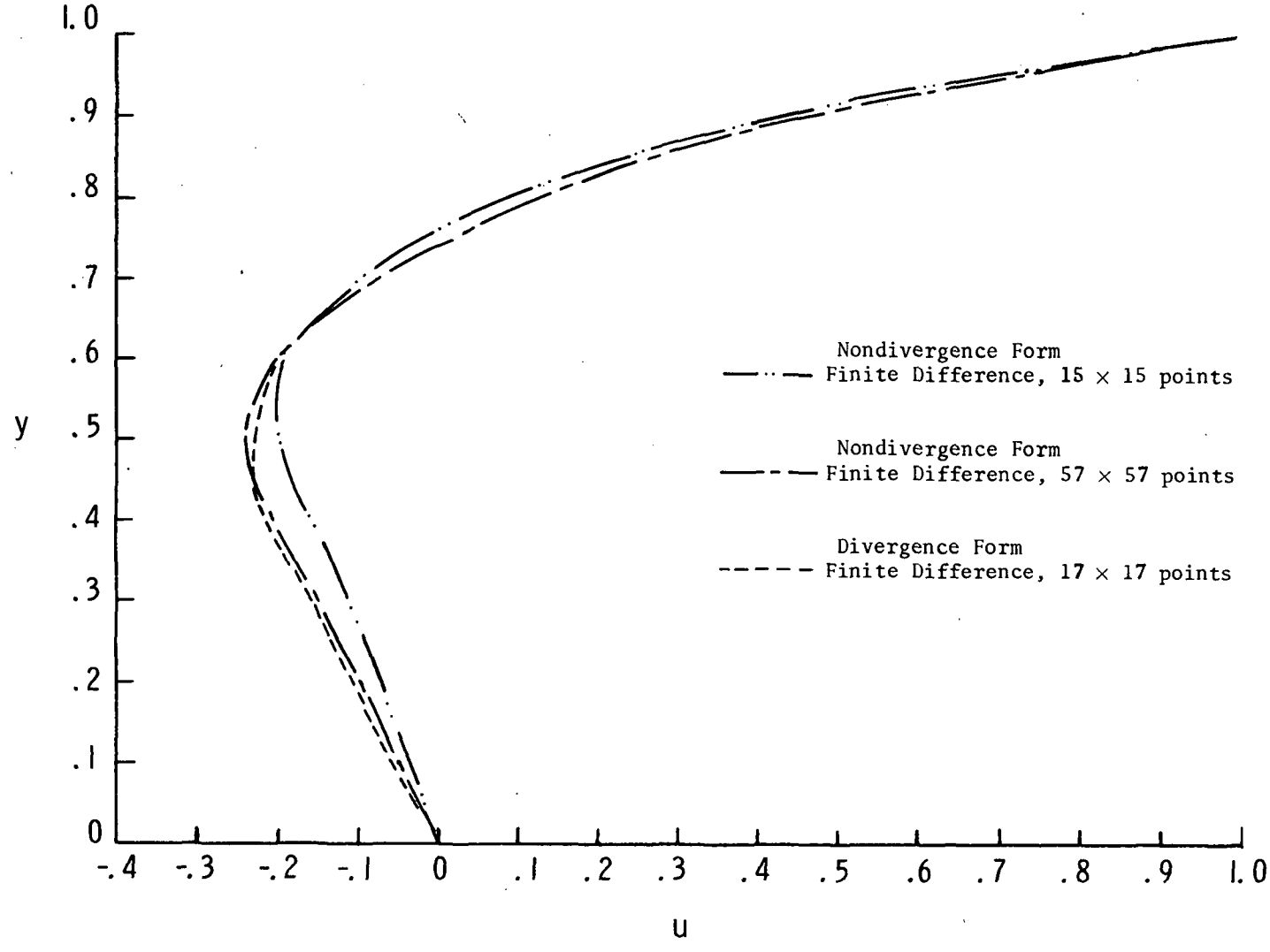

Figure 2.- Calculated velocity component u through point of maximum ψ. R = 100.

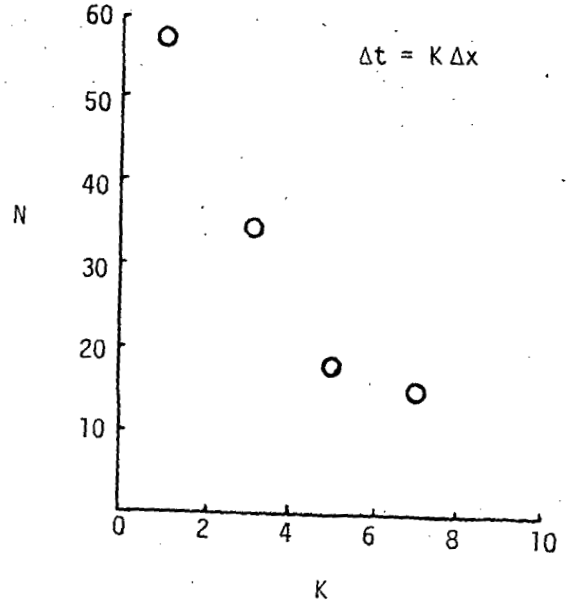

Figure 3.- Effect of number of nodal points (N × N) on time step.